Robotica: (2019) volume 37, pp. 2195–2208. © Cambridge University Press 2019
doi:10.1017/S0263574719000328

IMU-Based Gait Phase Recognition for Stroke Survivors

Yu Lou†§, Rongli Wang‡§, Jingeng Mai†§¶, Ninghua Wang‡§ and Qining Wang†§¶*

†*The Robotics Research Group, College of Engineering, Peking University, Beijing 100871, China. E-mails: louyu@pku.edu.cn, jingengmai@pku.edu.cn*
‡*Department of Rehabilitation Medicine, First Hospital, Peking University, Beijing 100034, China. E-mails: wangrongli2004@163.com, wangninghua2003@163.com*
§*Beijing Engineering Research Center of Intelligent Rehabilitation Engineering, Beijing 100871, China*
¶*Beijing Innovation Center for Engineering Science and Advanced Technology (BIC-ESAT), Peking University, Beijing 100871, China*

(Accepted March 2, 2019. First published online: April 10, 2019)

SUMMARY
Using wearable robots is an effective means of rehabilitation for stroke survivors, and effective recognition of human motion intentions is a key premise in controlling wearable robots. In this paper, we propose an inertial measurement unit (IMU)-based gait phase detection system. The system consists of two IMUs that are tied on the thigh and on the shank, respectively, for collecting acceleration and angular velocity. Features were extracted using a sliding window of 150 ms in length, which was then fed into a quadratic discriminant analysis (QDA) classifier for classification. We recruited five stroke survivors to test our system. They walked at their own preferred speed on the level ground. Experimental results show that our proposed system has the ability of recognizing the gait phase of stroke survivors. All recognition accuracy results are above 96.5%, and detections are about 5–15 ms in advance of time. In addition, using only one IMU can also give reliable recognition results. This paper proposes an idea about the further research on human–computer interaction for the control of wearable robots.

KEYWORDS: Exoskeletons; Human biomechanics; Man–machine systems; Mechatronic systems; Control of robotic systems.

1. Introduction

Stroke is a disease characterized by cerebral ischemic or hemorrhagic injury as the main clinical manifestation, with extremely high mortality and disability rate. According to World Health Organization, 15 million stroke patients are newly diagnosed each year, 5 million of which are permanently disabled.[1] Only 23–31% of stroke survivors are able to walk independently during the first week.[2] But after 6 months of rehabilitation training, this figure may be as high as 85%.[3] It can be seen that motion rehabilitation is an effective part of medical treatment for stroke survivors. Recently, wearable robots have shown great potentials in rehabilitation training and physical movement assistance.[4]

The exoskeleton is a typical representative of wearable robots, especially widely used in rehabilitation engineering. For example, Colombo et al. developed a driven gait orthosis (DGO) that can move the legs of a patient in a physiological way on the moving treadmill.[5] Hesse et al. developed

Yu Lou and Rongli Wang contributed equally to this paper.

* Corresponding author. E-mail: qiningwang@pku.edu.cn

https://doi.org/10.1017/S0263574719000328 Published online by Cambridge University Press

a gait trainer which can simulate the phases of gait, support the subjects according to their abilities, and control the center of mass (CoM) in the vertical and horizontal directions.[6] Burgess et al. found that self-selected overground walking speed was facilitated when a small percentage of body weight support (BWS) was provided for people post stroke.[7] For most stroke survivors, they develop hemiplegia after stroke and have walking difficulties but have not completely lost their motor ability. If users and exoskeletons can coordinate, independent walking can be completed. In addition, if the user and the exoskeleton do not cooperate in time, it may lead to safety issues. Therefore, how to make users and exoskeletons better coordinated is a great challenge that need to be solved.

At present, gait analysis for stroke patients mainly focuses on classification (patients or healthy subjects, or terrain recognition), walking ability rating, or symmetry assessment. Patterso et al. studied the most common spatial-temporal gait symmetry expressions to describe post-stroke gait and put forward recommendations on the most appropriate standardized measures.[8] Kotiadis et al. used the method of threshold techniques to accurately detect level walking, rough terrain, and carpet walking using data from accelerometers and gyroscopes.[9] However, only a few studies have been made on gait phase detection which is very important in the control of wearable robots.

In the context of lower-limb rehabilitation, the most important step is to accurately and reliably determine the user's gait phase information, including gait event and gait phases, to identify the human motion intentions and to convey accurate information to the lower-limb exoskeleton/orthotic devices for further commands or operations. In order to detect and identify the gait phase, researchers carried out a lot of studies. The most common ones are the following three forms. Researchers often record the activity information of the lower extremities by using inertial signals (e.g., acceleration, angular velocity),[11–14] and then use algorithms to classify or detect. In addition, heel switches and footswitches are also widely used.[15–18] Researchers use pressure insoles to measure pressure for gait phase transition. The third category is to collect the user's surface electromyography (sEMG), a direct measurement of human muscle excitability,[19–21] to achieve the purpose of gait phase recognition. Considering these proposed measurement methods, pressure insoles are usually made of several force sensitive resistors (FSRs), and therefore it has a specific but short life span. Also, insoles need to be specifically tailored for different sizes of feet. For sEMG sensor, it is not suitable for patients with limb insufficiency because the sensor is acquired to be attached to the skin surface to measure muscle activities. IMU overcomes these shortcomings. Its use scenario is more extensive and can be attached to not only the skin but also the surface of external equipments, for example, prosthetic limbs and exoskeletons. It has to say that compared to the pressure insole, IMU has better durability. Considering practicality and convenience, we chose IMU as our sensor, which has the advantages of flexibility and reusability.

However, the detection and recognition of gait phase are usually focused on healthy subjects. We hope to develop a system that could help the walking ability rehabilitation of stroke survivors. Therefore, in this paper we designed an inertial measurement unit (IMU)-based gait phase recognition system that can not only assess the users gait symmetry but also continuously detect gait phase. A further step than existing research is that this system can provide control signals according to the recognition results. Another innovation is that these control signals can be delivered to the assistive devices for better cooperation between users and devices. Two IMUs were arranged on the thigh and on the shank, respectively, which were considered as data resources. We employed the signals of pressure insole as reference data to confirm the accuracy of detection, because plantar pressure threshold technique for gait phase detection is a well-established method. During walking, a set of data was sampled every 10 ms. After data acquisition, feature values were extracted. Then a QDA classifier was trained for further detection test. We recruited five stroke survivors of varying walking hemiplegia for experimental trials. Finally, results show that our proposed system is accurate and reliable.

2. Method

2.1. IMU-based system

Here we used two IMUs, which were designed by our team. Each IMU contains a triaxial accelerometer and a triaxial gyroscope. After data acquisition and preprocessing, we can calculate the angles of the IMU (yaw angle, pitch angle, roll angle), triaxial angular accelerations, and triaxial accelerations,

https://doi.org/10.1017/S0263574719000328 Published online by Cambridge University Press

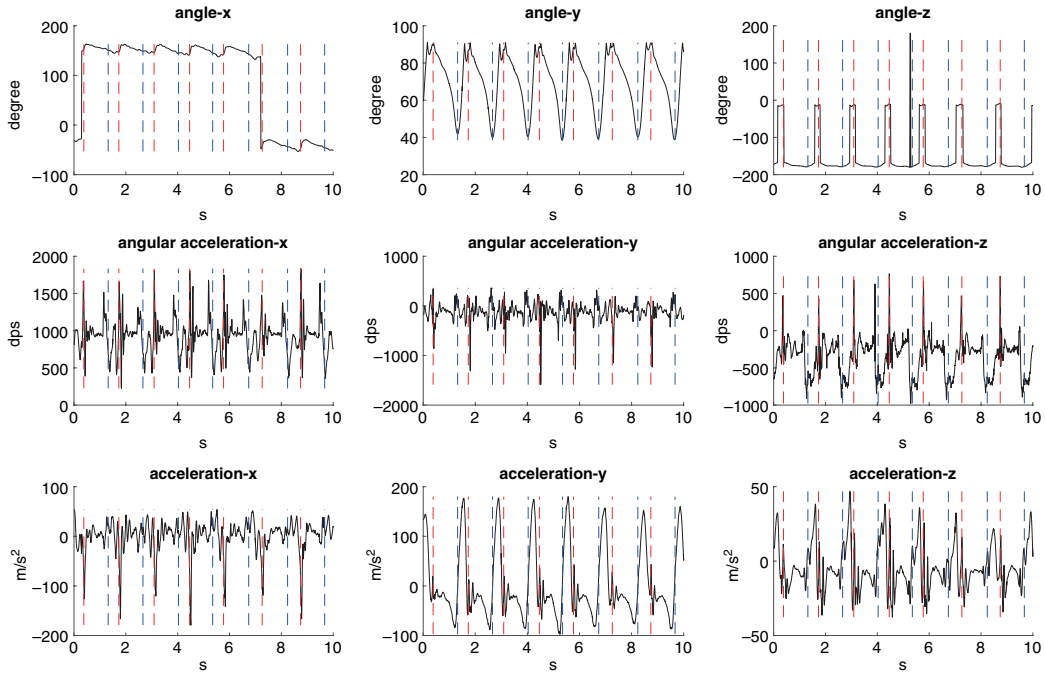


Fig. 1. The IMU signals of the stroke-affected ipsilateral lower limb in stable walking. The red dotted lines represent toe off and the blue dotted lines indicate foot contact. The data between two adjacent blue dotted lines represents motion information during a gait cycle.

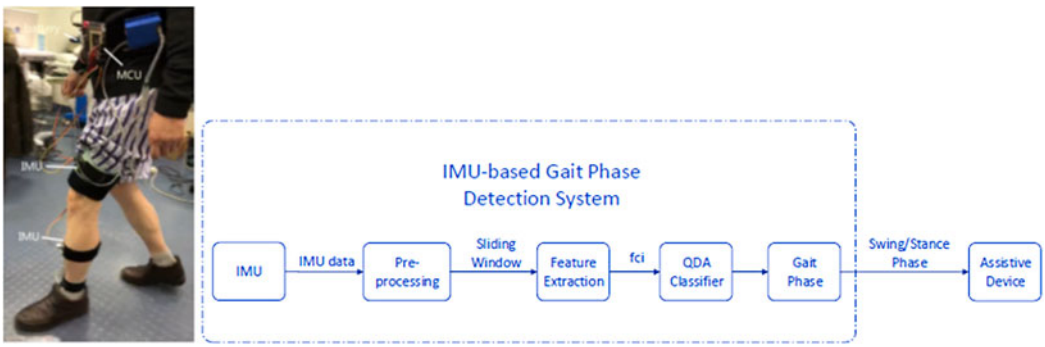


Fig. 2. The left subfigure is a wear schematic of a subject. The thigh and the shank were tied with an IMU, respectively. The battery and MCU were tied around the waist for system power supply and data acquisition. It records the gait phase changes in a gait cycle, including toe off, heel strike, and other important gait events. The subject sometimes shuffled his foot when walking. The right subfigure displays the workflow of our work. The signals are collected by the IMU tied on the thigh or on the shank. After preprocessing, a 150-ms long sliding window is used to extract the features. The resulting features are then fed into the QDA classifier, and the system classifies the current swing phase or stance phase. It is expected to generate a control signal to control the wearable robot.

respectively, as shown in Fig. 1. This information can characterize the user's position, current gait phase, and change trend during motion. Based on the motion patterns of walking and the ease of installation of combining with wearable equipments such as exoskeletons, prostheses, etc., we considered employing two IMUs on the thigh and on the shank, respectively. The IMUs were fixed on the thigh and on the shank by an adjustable strap. Refer to Fig. 2 for details. According to the report of subjects , the placement of the IMUs did not affect their gait during walking.

2.2. Experiment protocol

We recruited five stroke survivors to test our system, including three men and two women. They have an average age of 52.6 ± 16.9 years, an average height of 163.2 ± 7.0 cm, an average weight of 68.0 ± 13.5 kg, and an average time of 17.6 ± 30.8 months following stroke. They all had been engaged

https://doi.org/10.1017/S0263574719000328 Published online by Cambridge University Press

Table I. Basic information of subjects.

Subject no.	Gender (M/F)	Age (year)	Height (cm)	Weight (kg)	Time post stroke (month)	Level
1	M	39	163	85	2	5
2	M	65	175	74	1.5	3
3	F	32	158	48	72	5
4	F	72	158	65	12	4
5	M	55	162	68	0.5	4
Mean ± STD		52.6 ± 16.9	163.2 ± 7.0	68.0 ± 13.5	17.6 ± 30.8	

in rehabilitation exercises in the hospital during the recovery period after diagnosis. The demographic information of five subjects is shown in Table I. We used the Functional Ambulation Category Scale (FAC),[10] a functional walking test that evaluates ambulation ability, to assess ambulation status by determining how much humanitarian supports the subjects need when walking, regardless of whether or not they need personal assistive devices. The ratings of the patients were judged by experienced physiotherapists, according to their different levels of walking ability. For safety and convenience considerations, stroke survivors of injuries were not selected. Five subjects we recruited were involved three levels: 3, 4, and 5. The specific assessment criteria for these levels are as follows:

- Level 3: Patients do not need other direct physical support while exercising.
- Level 4: Patients can walk independently on level ground, but need help in going up and down stairs or downhill and uneven roads.
- Level 5: Patients can walk independently.

Before each experiment, we told the participants what experiments they needed to perform and what kinds of situations might exist. Each participant wore two IMUs and a pressure insole. IMUs and straps could be reused. The MCU and battery were tied to the waist, which can be seen in Fig. 2 for details. They were asked to walk 10 rounds back and forth in a 10-m-long flat hallway, with their preferred walking speeds. In the course of the experiment, we kept good communication with subjects, and subjects may request to interrupt the experiment for rest if anything was going wrong at any time. Throughout the entire process, we try to minimize walking assistance to the participants. Each subject's paretic limb and non-paretic limb were tested and evaluated separately, and comparative analysis was performed in the analysis of future results. We selected the portion of each round trip that moves at a constant speed, removing the acceleration period at the beginning of the trial and the deceleration period at the end of the trial. The artificially abnormal gait cycles in walking had also been removed.

What needs to be pointed out in particular is that the subject 3 suffered from hemiplegia on both legs.

A cycle of walking postures is shown in Fig. 3. The figure shows some key gait events such as toe off and heel strike. In fact, we actually need to detect these events and learn about the gait phase, so as to provide accurate, real-time, and effective information for further research and development.

In order to verify the accuracy and stability of the IMU-based system for gait phase detection, we used the most widely used plantar pressure threshold technique method for accuracy reference. We made a pair of foot pressure insoles, namely, four FSR sensors were embedded in the plantar insole. In addition, we used an insole with four FSRs, which were embedded under the toe, heel, first metatarsal head, and the position between the forth and fifth metatarsal heads. The use of pressure insoles was described in ref. [23] The measured pressure data from the plantar pressure insoles were regarded as reference signal, to compare the results from the IMU signal (resource signal) and verify the reliability of the IMU-based system. The plantar pressure signal was the sampled synchronously with the IMU signal. Two kinds of signals were both sent to the MCU via the UART, and then passed to the PC through the WIFI. The sampling frequency was 100 Hz.

https://doi.org/10.1017/S0263574719000328 Published online by Cambridge University Press



Fig. 3. Recording the gait phase changes in a gait cycle, including toe off, heel strike and other important gait events. The subject sometimes shuffled his foot when walking.

2.3. Model architecture

The workflow in this article is shown in Fig. 2. It was based on two ideas: firstly, we obtained IMU data through the data preprocessing, feature extraction, and classifier training to optimize our gait phase detection system. Secondly, the plantar pressure data were used as a reference signal and detected by the threshold technique. Gait phase was compared between the gait phase identified by our system and the pressure data. Finally, the accuracy and delay time of the system were evaluated.

2.4. Recognition process

After obtaining the IMU signal and plantar pressure data, we first separated the IMU from the plantar pressure data. Plantar pressure data were used to generate referential gait events toe off and heel strike, and the gait was detected as swing phase or stance phase. The label of features was determined by the signals from pressure insole. Then IMU signal was extracted, followed by which the data were segmented by using a sliding window of 150 ms in length. Features were calculated as equations. Then features and the label were simultaneously fed into the classifier to train the classifier.

For the sake of effectiveness and simplicity of the classifier training, we designed a five time-domain feature for IMU signals, which can be expressed as

$$f(c_1) = Avg(X) \tag{1}$$

$$f(c_2) = Std(X) \tag{2}$$

$$f(c_3) = Max(X) \tag{3}$$

$$f(c_4) = Min(X) \tag{4}$$

$$f(c_5) = sum(abs(Diff(X))), \tag{5}$$

where $f(c_i)$ are the extracted features, $i = 1, 2, ..., 5$, and X is a data matrix in a sliding window, whose dimension is $N \times M$, with N being the sliding window length (the length of data) and M the channels of the IMU signals (M is 18 when all the signal channels are included). Features of each channel were calculated separately and then set up to a vector, that was, the features $f(c_i)$ were calculated in the X column direction.

- Avg (X) is the mean value of X;
- Std (X) is the standard deviation of X;
- Abs (X) is the absolute value of X;
- Diff (X) is the difference between X.

https://doi.org/10.1017/S0263574719000328 Published online by Cambridge University Press

Finally, all the features were combined into a 90-dimensional feature vector, in which the thigh took up 45 dimensions (nine channels into IMU signals and five features per channel) and the shank in a similar way.

At the same time, we used plantar pressure signal to set label on the above feature vector. Since the sampling interval was 10 ms, a 150-ms long sliding window contained 15 frames of data. Taking the characteristics of the gait phase transition into account, we determined the corresponding label value of the window based on the number of frames occupied by each phase. For example, in a 150-ms long sliding window, if there existed six frames of data belonging to the swing phase and the remaining nine frames of data belonging to the stance phase, we marked it as the stance phase. After label vector was completed, the data were divided into 10 folds, of which 9 folds were fed to quadratic discriminant analysis (QDA) classifier and the remaining one for a leave-one-out cross validation (LOOCV) for further evaluation.

2.5. Evaluation

In order to qualitatively and quantitatively analyze the reliability and practicality of our proposed system, we came up with the following series of methods of verification. For qualitative observations, we observed raw plantar pressure data and IMU signal. In the stage of comparing recognition results, check the continuous recognition results. For quantitative analysis, we compared the gait phase time of paretic limbs and non-paretic limbs, as well as temporal symmetric index. The idea of data analysis was to use a sliding window to extract features of the preprocessed data, and feed the features into the classifier model to form a classifier. The features were selected using a Greedy Algorithm, that is, every time we made a current best choice. In the selected feature vector set, if adding an one-dimensional feature vector made the accuracy rate highest, we chose this vector. The work we did was to find this local optimal solution one by one, until the accuracy rate was reduced when more features were added. In order to improve data utilization, the accuracy of the recognition employed a 10-fold cross validation (10-fold LOOCV) method. Each time nine pieces of data were taken out to train the QDA classifier, and the remaining one piece of data was tested for the trained classifier. If the output of the classifier is the same as the reference label, it is marked as 1 (successfully detected), otherwise it is marked as 0 (failed), which is shown in Eq. (6). Accuracy is the average value of this set of data.

$$f(x_i) = \begin{cases} 1 & x_i = y_i \\ 0 & x_i \neq y_i, \end{cases} \tag{6}$$

where x is the output of QDA classifier, while y is the label from reference data. When the output of the classifier coincides with the plantar pressure label, we assigned $f(x)$ to 1, otherwise 0 was assigned. Comparing the detection results of gait phase detection system with the label of plantar pressure, we calculated the correctness and reliability of the system. The accuracy rate was calculated as follows:

$$accuracy = \frac{1}{n} \sum_{i=1}^{n} f(x_i), \tag{7}$$

where n is the length of the data, that is, the number of frames. This value represents the accuracy of the system.

To make the result more reliable, the 10-fold data were cross-checked and an average value was finally calculated to reduce the possibility of random errors. In the calculation, the IMU attached to the paretic limb and the non-paretic limb was considered separately and combined to see if there was a performance increase.

3. Experimental Results

3.1. Initial IMU signal

Figure 1 displays the IMU signals of the affected paretic lower limb and the healthy lower limb in stable walking, respectively. The red dotted lines represent toe off and the blue dotted lines indicate

https://doi.org/10.1017/S0263574719000328 Published online by Cambridge University Press

Table II. Temporal gait parameters.

	Stance/stride		Swing/stride		Intra-limb SW/ST	
Subject no.	**Paretic**	**Non-paretic**	**Paretic**	**Non-paretic**	**Paretic**	**Non-paretic**
1	0.6985	0.7775	0.3015	0.2225	0.4317	0.2862
2	0.7335	0.7840	0.2666	0.2160	0.3634	0.2755
3	0.6871	0.7516	0.3128	0.2484	0.4552	0.3305
4	0.6719	0.6687	0.3281	0.3314	0.4883	0.4956
5	0.7326	0.7190	0.2674	0.2810	0.3650	0.3909

foot contact. Between every two blue dotted lines is a gait cycle. From the figure, we can observe that most channels have regular performance so that they can be used for subsequent experimental results processing.

3.2. Gait symmetry

Our system has the ability of assessing gait symmetry. In data preprocessing, we calculated some indicators of the gait symmetry of five stroke survivors. Considering gait asymmetry after stroke and the differences between individuals, we identified heel strike and toe off events separately for each individual. The stance phase is the gait phase between heel strike and toe off event, while the swing phase is the gait phase between the toe off and the next heel strike event, and stride time refers to the time between the current and next heel strike event. Due to the patient's personal habits and external environmental conditions, the walking speed may be inconsistent. We chose parameters: swing time/stride time, stance time/stride time, and intra-limb ratio of SW/ST measured in the experiment, which are commonly used in gait symmetry assessment. The proportion of swing time/stride time, stance time/stride time, as well as intra-limb SW/ST ratio throughout the gait cycles are listed in Table II.

Except to the time spent by the stance phase, gait symmetry is also an aspect that physiotherapists focus on during the rehabilitation process. Researchers in gait symmetry have many factors that have been investigated, mainly in terms of time and space. Under the research guide of Patterson et al.,[8] symmetry ratio (SA) and symmetry index (SI) can be used to describe gait symmetry. They are defined as

$$Symmetry\ ratio\ (SA) = \frac{V_{\text{paretic}}}{V_{\text{non-paretic}}} \tag{8}$$

$$Symmetry\ index\ (SI) = \frac{V_{\text{paretic}} - V_{\text{non-paretic}}}{0.5(V_{\text{paretic}} + V_{\text{non-paretic}})} \tag{9}$$

where V_{paretic} represents the proportion of time occupied by the stance phase of the paretic limb throughout the gait cycle, while $V_{\text{non-paretic}}$ stands the proportion of time spent by the stance phase of the non-paretic limb throughout the gait cycle.

For normal gait, symmetry ratio (SA) should be equal to or approximately equal to 1, with a positive value indicating the symmetry of walking. The more deviating from 1 is, the more asymmetrical the gait is. The SI also reflects the user's gait symmetry, with a value near to 0 that can be positive or negative representing which leg the patient is inclined to. In our experiments, most subjects (No. 1, 2, 3, and 5), they spent more time on the stance phase, comparing the non-paretic limb with the paretic limb. Correspondingly, during the swing phase, they spent less time on non-paretic limb. For the SW/ST time ratio of intra-limb, we can see from Table II, in many cases, the ratio of paretic limb to non-paretic limb is higher. As for the stride time, the non-paretic limb side lasted slightly longer.

Our experimental results show that the five stroke survivors have more or less different degrees of gait asymmetry. From the SA and SI indicators, in most cases, their paretic limbs spend less time in the stance phase, so that the SA is usually less than 1 and the SI is less than 0. Similarly, intra-limb SW/ST-based values of SA and SI also show this trend. This finding indicates that our system has the ability of quantitatively assessing gait asymmetry.

https://doi.org/10.1017/S0263574719000328 Published online by Cambridge University Press

Table III. Gait symmetry assessment according to temporal parameters.*

	Stance time		Swing time		Stride time		Intra-limb SW/ST	
Subject no.	**SA**	**SI**	**SA**	**SI**	**SA**	**SI**	**SA**	**SI**
1	0.9179	−8.56%	1.3846	32.26%	1.0217	2.15%	1.5085	40.54%
2	0.8552	−15.61%	1.1284	12.06%	0.9141	−8.97%	1.3194	27.54%
3	0.9018	−10.32%	1.2422	21.60%	0.9865	−1.36%	1.3774	31.75%
4	1.0307	3.02%	1.0155	1.54%	1.0257	2.54%	0.9852	−1.49%
5	0.9228	−8.03%	0.8616	−14.86%	0.9056	−9.91%	0.9337	−6.85%

*The data in Table III is calculated from the data in Table II.

3.3. Accuracy

For our proposed gait phase detection system, we need to compare the detection results with the true gait phase to make sure the reliability and accuracy of the system. For each subject, the IMU signals from the location of thigh or shank were processed separately to establish QDA classifiers. The recognition results were recorded according to the classification algorithm. In order to evaluate the differences of the IMU position on the recognition result, we also separately processed the data of the two IMUs to compare the performance of a single IMU with two IMUs.

The accuracy results are shown below.

3.3.1. Both thigh and shank. When we focus on both IMUs, the accuracy of classification is above 97%, regardless of whether one or two IMUs were used. In this respect, we claim that the IMUs have a very good discriminating function for gait phase detection, which leads to a quiet reliable accuracy. In comparison of the paretic limb and non-paretic limb recognition, there is a slight difference between individuals, but the difference is not particularly distinctive. For each subject, there is a better recognition result when employing two IMUs.

3.3.2. Thigh only. When considering only one IMU tied on the thigh, the gait phase detection results are also satisfactory, which are slightly lower than that of two IMUs, but at least ensured the accuracy higher than 96.5%. For example, for subject 1, making use of IMU data on the thigh has a recognition rate of 98.22% (paretic limb) and 96.57% (non-paretic limb), while that using two IMUs is 98.50% (paretic limb) and 97.09% (non-paretic limb), respectively. The recognition results have a slight increase, 0.28% for paretic limb and 0.52% for non-paretic limb. Other subjects' test results are similar.

3.3.3. Shank only. When taking considerations of the signal from the shank, the recognition results are comparable to that from the thigh. On the paretic limb, the IMU on the shank performs better and the recognition rate is higher. However, for the non-paretic limb, the IMU on the shank is at a disadvantage, and the recognition rate cannot catch up with that on the thigh (subjects 2, 4, 5). However, regardless of which IMU has more independent performance, their recognition results are within an acceptable range. For the group of the largest gap, subject 5, on the non-paretic limb, the correct rate was 98.38% (thigh) and 96.62% (shank). Both results have reached 96.5% and are acceptable.

3.4. Continuous recognition results

The accuracy rate can represent the situation of single recognition, but we want to examine the continuous recognition capabilities of the system. Therefore, after preprocessing, the data are fed into the QDA processor to observe its pseudo real-time recognition results and evaluate its continuous recognition ability. This is a method of qualitative analysis of the system.

From Fig. 4, the system output is very stable in terms of continuous recognition. The performances during the swing phase and stance phase are both very robust. When walking in swing or stance phase, almost all cases can be accurately identified. Only at the time of transition, there are some cases of identifying errors. During phase transition, the characteristics of both phases exist at the

https://doi.org/10.1017/S0263574719000328 Published online by Cambridge University Press

Table IV. Confusion matrix of paretic limb (subject no. 5).

	Swing phase	**Stance phase**
Swing phase	98.51%	1.49%
Stance phase	1.83%	98.17%

Table V. Confusion matrix of non-paretic limb (subject no. 5).

	Swing phase	**Stance phase**
Swing phase	98.71%	1.29%
Stance phase	1.61%	98.39%

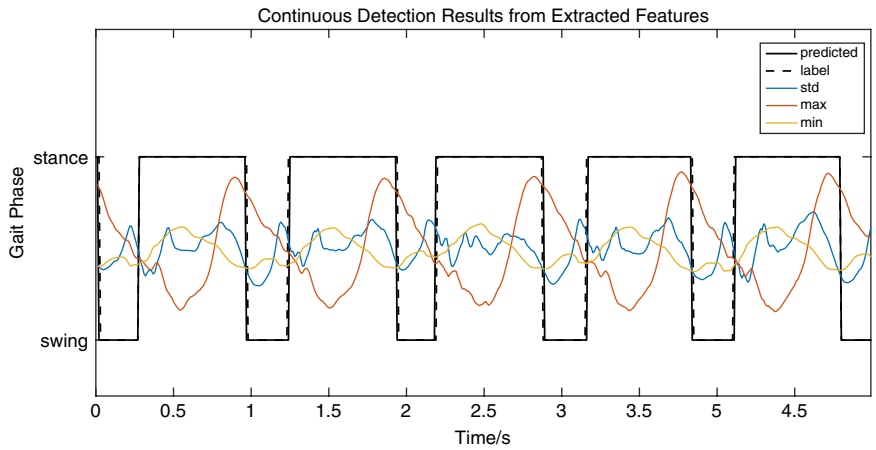


Fig. 4. The continuous recognition results within 5 s from the features extracted from the original IMU data. The black dashed line represents the recognition result of the proposed system. The solid black line represents the reference label.

same time, leading to a recognition error. However, the recognition error only exists in the gait phase transition phase and does not last long.

The results shown in Fig. 4 indicate that the proposed system is quite real-time, and most of the recognition is in advance. The black dashed line represents the recognition result of our proposed system. The solid black line represents the reference label, and the remaining lines represent the three features std, max, and min extracted from the original IMU data. We will show the advance/delay time in the later results.

3.5. Confusion matrix

In addition to system recognition accuracy considerations, we considered whether the swing phase was identified as a stance phase or the stance phase was identified as a swing phase, in order to improve our system design. Therefore, the confusion matrix was included in our investigation.

The confusion matrix is composed of 2×2 four elements. The diagonal line indicates the probability that the swing phase or stance phase is correctly recognized. The lower left corner element is the possible case where the stance phase is identified as swing phase, and the lower right corner element is the possible case where the swing phase is detected as stance phase.

It can be seen from Tables IV and V that the error rate of the confusion between the swing phase and the stance phase is almost the same, which is 1.83% and 1.49% (paretic limb) and 1.61% and 1.29% (non-paretic limb), respectively. The recognition of the correct situation is about 98%, indicating that our system has enough judgment ability for gait phase detection.

In order to rule out the contingency of the above results, we also used statistically common true positive rate (TPR) to assess the results of five subjects. The indicators examined are accuracy, precision, sensitivity, specificity, and negative prediction. The results obtained are shown in Table VI.

https://doi.org/10.1017/S0263574719000328 Published online by Cambridge University Press

Table VI. Average true positive rate of five subjects.

	Accuracy	**Precision**	**Sensitivity**	**Specificity**	**Negative prediction**
Paretic limb	97.77%	97.72%	97.82%	97.72%	97.82%
Non-paretic limb	98.08%	98.18%	97.98%	98.18%	97.99%

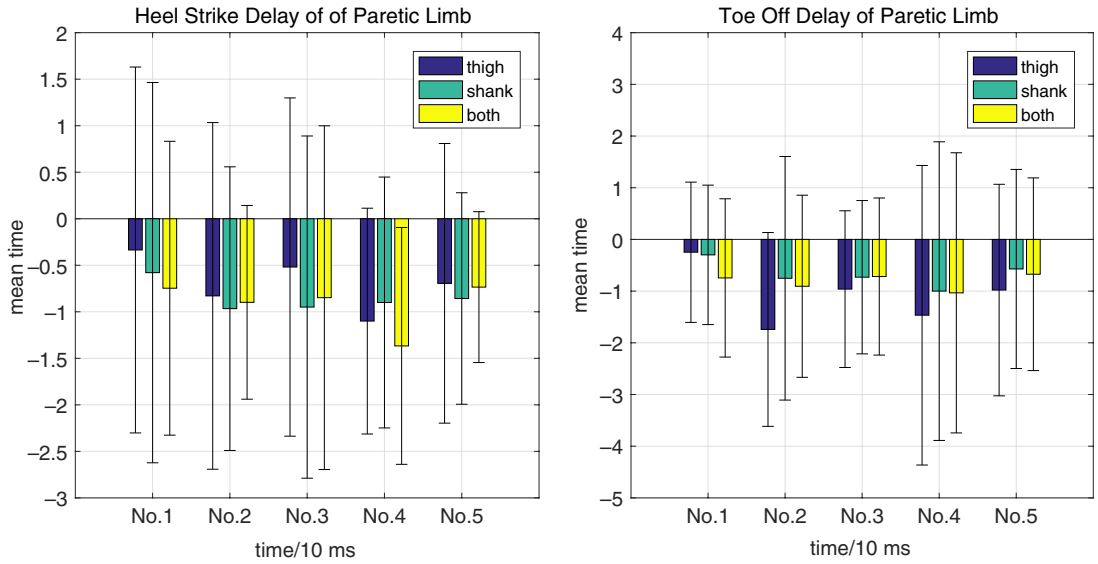


Fig. 5. The delay time of the heel strike event detection system proposed by ourselves for the paretic limb. Bars represent the mean advance/delay time for all strides for each subject, and the solid black line indicates the standard deviation.

3.6. Advance/Delay time

Although system accuracy is a very important reliability indicator, the advance/delay time of the system is equally important, especially when this gait phase detection system is to be used as a control signal of external wearable rehabilitation equipments. If the system can provide a correct control signal, as well as reliable, stable gait event transitions, then the system can be promoted for the next period of wearable robot integration. The content of this section is based on the delay of quantitative considerations on system availability.

A stable and efficient identification system not only needs to have a good advanced recognition margin to supply the time required for the operation of the motion, but also has the stability of advance/delay identification. In terms of identification stability, we extracted the recognition advance/delay time of each subject and calculated the standard deviation. The mean time and standard deviation is calculated in Figs. 5 and 6.

The recognition results of Figs. 5 and 6 show that, overall, whether it is heel strike or toe off, our system can recognize gait events in advance. The amount of advance time is related to the individual and the location of the IMU, which is about 5–15 ms. For swing-to-stance transition, the combination of the IMU on the shank and the two IMU combination shows better early performance for paretic limb, and the IMU on the thigh for non-paretic limb. For the transition from stance to swing, the IMU on the thighs is even better.

4. Discussion

For the IMU raw signal, we found a very regular periodic signal. The physical meaning of the original signal of the IMU is clear, and the viewing is convenient. Also, the current gait phase of the subject can be quickly and qualitatively checked. Although the symmetry rating is not the focus of our research, but it is worth mentioning that the system we proposed has a certain ability to assess the gait symmetry of users.

https://doi.org/10.1017/S0263574719000328 Published online by Cambridge University Press

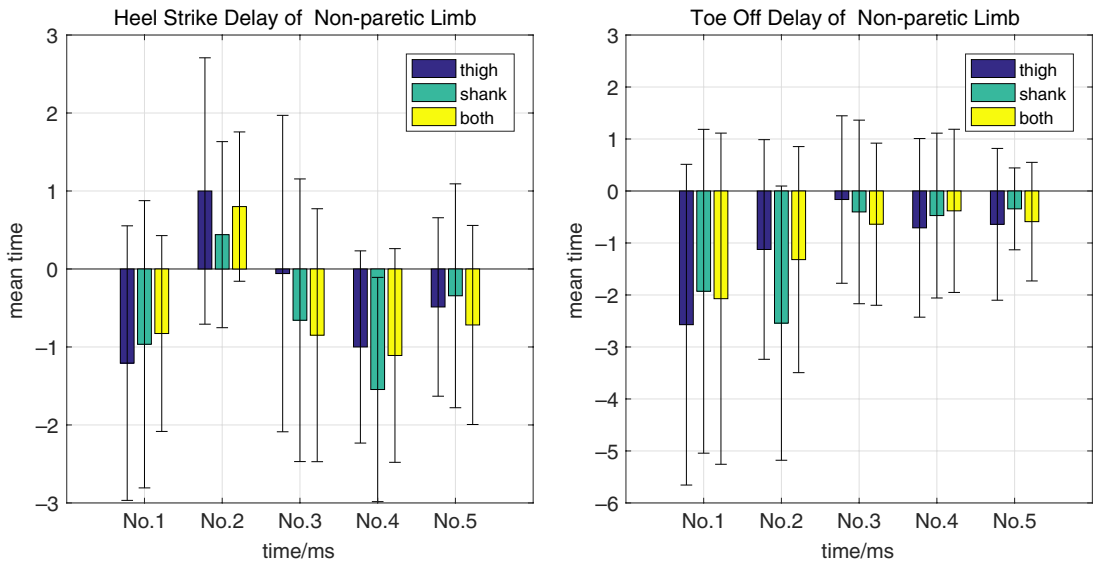


Fig. 6. The delay time of the toe off event detection system proposed by ourselves and for the non-paretic limb. Bars represent the mean advance/delay time for all strides for each subject, and the solid black line indicates the standard deviation.

According to the study mentioned in ref. [22], Balaban et al. concluded that temporal asymmetry in hemiplegic gait is commonly described quantitatively as a prolonged paretic swing time and/or a prolonged non-paretic stance time compared with the contralateral limb. For most stroke survivors, the stance phase time of the paretic limb shortens, and the stance phase of the non-paretic limb increases. In actual, the detection results of subjects 1, 2, 3, and 5 satisfy this rule. However, the result of the test of subject 4 is somewhat unexpected. She spent almost the same stance phase time and swing phase time on both legs, with no significant difference. We speculate that this may be due to the better recovery of her gait, resulting in better gait symmetry. In our experiments, there are some differences due to the different timing of stroke diagnosis, different levels of rehabilitation, and difficulties in uniform walking speed. But in general, it accords with the asymmetry characteristics of gait after stroke. Patterson[8] and his colleagues studied a group of stroke survivors based on parameters: swing time, stance time, and SW/ST. Their SA is 1.24, 1.09, and 1.38 and SI is 18.61%, 31.58%, and 26.12%. Our findings are similar to this conclusion. However, there are some discrepancies in the stance-based SA value, possibly due to a limited number of participants in our research. The asymmetry of stroke survivor varies from person to person.

Generally, the system's recognition accuracy rate is quite high, and it is higher than 96%, whether it is a single IMU or a combination of two IMUs. For each subject, the location of the IMU (thigh or shank) does not have a significant effect on the recognition result. For example, for Subject 2, the results of two IMUs tied on the paretic limb are 97.08% (thigh) and 97.76% (shank), and the results of two IMUs tied on the non-paretic limb are 97.54% (thigh) and 97.43% (shank), respectively. From this point of view, the recognition rate of the IMU signal tied on the shank is slightly higher than that tied on the thigh, but the difference is negligible. For other subjects, this law also exists, which is shown in Figs. 7 and 8. For a single IMU or two combined IMUs, taking subject 4 as an example, the highest IMU identification rate on a single IMU is 98.12% (paretic limb) and 98.38% (non-paretic limb). The identification results combining two IMUs are 98.24% and 98.47%, respectively, only increased by 0.12% and 0.09%. The improvement was not significant. Compared with other subjects, this result also applies. With the support of these results, we can conclude that, for swing or stance gait phase detection, only one IMU can be applied. The combination of the two IMUs does not bring about a significant increase in accuracy, but rather increases the computing time to some extent.

The representation of continuous recognition results allows us to visually understand the recognition results in detail, and the recognition results are stable and have a certain advance time. This can be used in clinical diagnostics to monitor the user's real-time gait phase, thereby sending out control signals to assistive devices.

https://doi.org/10.1017/S0263574719000328 Published online by Cambridge University Press

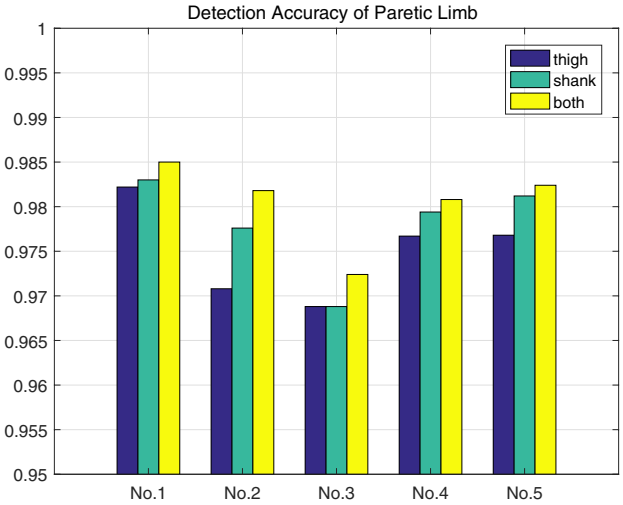


Fig. 7. A comparison result of the gait phase detection of the paretic limbs of the five subjects generated by the QDA classifier. Three situations are: only one IMU on the thigh, only one IMU on shank, and two IMU combination.

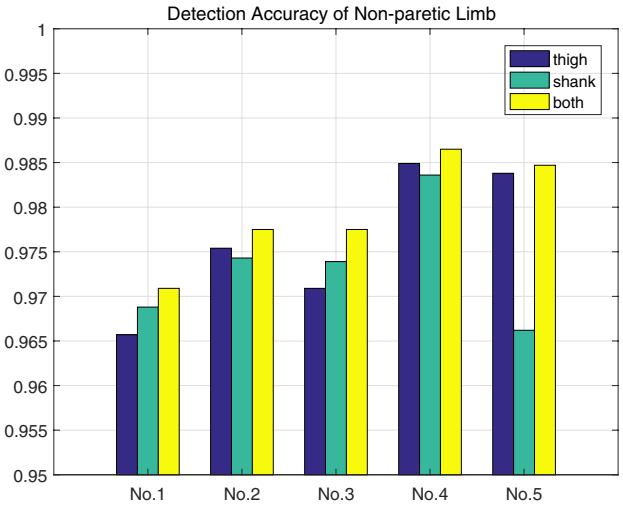


Fig. 8. A comparison result of the gait phase detection of the non-paretic limbs of the five subjects generated by the QDA classifier. Three situations are: only one IMU on the thigh, only one IMU on shank, and two IMU combination.

Detection accuracy and advance/delay time can be dialectically viewed. In the continuous recognition of the output results, the recognition within each gait phase is very robust, and the recognition error only occurs at the gait phase transitions. Regardless of the advance/delay recognition error condition, the identification is completely correct in each swing or stance phase. When the collected data are fed into the classifier, the system judges in advance that the gait phase switch will be generated according to the already trained model. However, the detection in advance will affect the detection accuracy to a certain extent. Therefore, in the specific use, the position and quantity of the IMU can be selected according to actual needs. For example, in some cases, the recognition results of two IMUs are high, but the time in advance of such placement is not the best, and it also brings computational complexity. The accuracy of IMU recognition placed on the thigh is slightly lower, but it achieves early recognitions.

Jung et al. proposed a gait phase classification method based on neural networks using the orientation of each lower-limb segment and the angular velocities of the joints from lower-limb exoskeleton robots.[11] They recruited seven healthy subjects and classified gait phase using the two neural network methods (a multilayer perceptron and nonlinear autoregressive with external inputs (NARX))

https://doi.org/10.1017/S0263574719000328 Published online by Cambridge University Press

method. Results show that the classification accuracy was about 97%, maximum continuous error 10–12 frames, and average delay/advanced mean and std error width 1.96±1.79 frames (every two frames were separated by 10 ms). However, our research for stroke survivors has almost the same accuracy, shorter error width, and more stable maximum continuous delay/advance time. Also, in most cases it is possible to identify motion intention in advance to leave enough time for assistive devices to react.

In our future research, we will continue to explore the universality of our proposed IMU-based gait phase detection system and will recruit more stroke survivors to validate our experimental results.

5. Conclusion

In this paper, we propose an IMU-based gait phase detection system for stroke survivors. The experimental results show that the system can be used to detect the gait phase of stroke survivors, which has been verified on five stroke survivors. The system also has the function of assessing gait symmetry. In the future, we will do further research on the integration between wearable robots and stroke survivors.

Acknowledgments

The authors would like to thank the anonymous reviewers for their valuable suggestions. This work was supported by the National Key R&D Program of China [grant number 2018YFC2001503], [grant number 2018YFB1307302]; the National Natural Science Foundation of China [grant number 91648207], [grant number 61533001]; the Beijing Natural Science Foundation [grant number L182001]; and the Beijing Municipal Science and Technology Project [grant number Z181100009218007].

References

1. J. Mackay, G. A. Mensah, S. Mendis and K. Greenlund, "The atlas of heart disease and stroke: World Health Organization" (2004).
2. H. P. von Schroeder, et al., "Gait parameters following stroke: A practical assessment," *J. Rehabil. Res. Develop.* **32**(1), 25–31 (1995).
3. D. T. Wade, et al., "Walking after stroke. Measurement and recovery over the first 3 months," *Scand. J. Rehabil. Med.* **19**(1), 25–30 (1987).
4. S. Mohammed, Y. Amirat and H. Rifai, "Lower-limb movement assistance through wearable robots: State of the art and challenges," *Adv. Robot.* **26**(1), 1–22 (2012).
5. G. Colombo, M. Joerg, R. Schreier and V. Dietz, "Treadmill training of paraplegic patients using a robotic orthosis," *J. Rehabil. Res. Develop.* **37**(6), 693–700 (2000).
6. S. Hesse and D. Uhlenbrock, "A mechanized gait trainer for restoration of gait," *J. Rehab. Res. Develop.* **37**(6), 701–708 (2000).
7. J. K. Burgess, G. C. Weibel and D. A. Brown, "Overground walking speed changes when subjected to body weight support conditions for nonimpaired and post stroke individuals," *J. Neuroeng. Rehabil.* **7**(1), 6–16 (2010).
8. K. K. Patterson, et al., "Evaluation of gait symmetry after stroke: A comparison of current methods and recommendations for standardization," *Gait Posture*. **31**(2), 241–246 (2010).
9. D. Kotiadis, H. J. Hermens and P. H. Veltink, "Inertial gait phase detection for control of a drop foot stimulator," *Med. Eng. Phys.* **32**(4), 287–297 (2010).
10. https://www.strokengine.ca/assess/fac/
11. J. Y. Jung, W. Heo, H. Yang and H. Park, "A neural network-based gait phase classification method using sensors equipped on lower limb exoskeleton robots," *Sensors*. **15**(11), 27738–27759 (2015).
12. B. Mariani, H. Rouhani, X. Crevoisier and K. Aminian, "Quantitative estimation of foot-flat and stance phase of gait using foot-worn inertial sensors," *Gait Posture*. **37**(2), 229–234 (2013).
13. M. S. Aung, S. B. Thies, L. P. Kenney, D. Howard, R. W. Selles, A. H. Findlow and J. Y. Goulermas, "Automated detection of instantaneous gait events using time frequency analysis and manifold embedding," *IEEE Trans. Neural Syst. Rehabil. Eng.* **21**(6), 908–916 (2013).
14. A. Mannini and A. M. Sabatini, "Gait phase detection and discrimination between walkingCjogging activities using hidden Markov models applied to foot motion data from a gyroscope," *Gait Posture*. **36**(4), 657–661 (2012).
15. X. Jiang, K. H. Chu, M. Khoshnam and C. Menon, "A wearable gait phase detection system based on force myography techniques," *Sensors*. **18**(4), 1279–1291 (2018).
16. K. Kong and M. Tomizuka, "A gait monitoring system based on air pressure sensors embedded in a shoe," *IEEE/ASME Trans. Mechatron.* **14**(3), 358–370 (2009).
17. F. Attal, Y. Amirat, A. Chibani and S. Mohammed, "Automatic recognition of gait phases using a multiple regression hidden Markov model," *IEEE/ASME Trans. Mechatron.* **23**(4), 1597–1607 (2018).

https://doi.org/10.1017/S0263574719000328 Published online by Cambridge University Press

18. S. Crea, M. Donati, S. M. M. De Rossi, C. M. Oddo and N. Vitiello, "A wireless flexible sensorized insole for gait analysis," *Sensors*. **14**(1), 1073–1093 (2014).
19. C. D. Joshi, et al., "Classification of Gait Phasesfrom Lower Limb EMG: Application to Exoskeleton Orthosis," *Proc. IEEE-EMBS Special Topic Conf. Point-of-Care Healthc. Technol.*, 228C-231 (2013).
20. S. W. Lee, T. Yi, J. W. Jung and Z. Bien, "Design of a gait phase recognition system that can cope with EMG electrode location variation," *IEEE Trans. Autom. Sci. Eng.* **14**(3), 1429–1439 (2017).
21. J. Ryu and D. H. Kim, "Real-time gait subphase detection using an EMG signal graph matching (ESGM) algorithm based on EMG signals," *Expert Syst. Appl.* **85**(1), 357–365 (2017).
22. B. Balaban and F. Tok, "Gait disturbances in patients with stroke," *PMR*. **6**(7), 635–642, (2014).
23. B. Chen, X. Wang, Y. Huang, K. Wei and Q. Wang, "A foot-wearable interface for locomotion mode recognition based on discrete contact force distribution," *Mechatronics*, **32**, 12–21 (2015).

https://doi.org/10.1017/S0263574719000328 Published online by Cambridge University Press